Article

On the Partition Temperature of Massless Particles in High-Energy Collisions

Wei-Liang Qian [1,2,3,*] **, Kai Lin** [1,4]**, Rui-Hong Yue** [1]**, Yogiro Hama** [5,*] **and Takeshi Kodama** [6,7]

1   Center for Gravitation and Cosmology, College of Physical Science and Technology, Yangzhou University, Yangzhou 225009, China; lk314159@hotmail.com (K.L.); rhyue@yzu.edu.cn (R.-H.Y.)
2   Escola de Engenharia de Lorena, Universidade de São Paulo, Lorena 12602-810, Brazil
3   Faculdade de Engenharia de Guaratinguetá, Universidade Estadual Paulista, Guaratinguetá 12516-410, Brazil
4   Hubei Subsurface Multi-Scale Imaging Key Laboratory, School of Geophysics and Geomatics, China University of Geosciences, Wuhan 430074, China
5   Instituto de Física, Universidade de São Paulo, C.P. 66318, São Paulo 05315-970, Brazil
6   Instituto de Física, Universidade Federal do Rio de Janeiro, C.P. 68528, Rio de Janeiro 21945-970, Brazil; tkodama@if.ufrj.br
7   Instituto de Física, Universidade Federal Fluminense, Niterói 24210-346, Brazil
*   Correspondence: wlqian@usp.br (W.-L.Q.); hama1936@gmail.com (Y.H.)

Abstract: Although partition temperature derived using the Darwin–Fowler method is exact for simple scenarios, the derivation for complex systems might reside in specific approximations whose viability is not ensured if the thermodynamic limit is not attained. This work elaborates on a related problem relevant to relativistic high-energy collisions. On the one hand, it is simple enough that closed-form expressions can be obtained precisely for the one-particle distribution function. On the other hand, the resulting expression is not an exponential form, and therefore, it is not straightforward that the notion of partition function could be implied. Specifically, we derive the one-particle distribution function for massless particles where the phase-space integration is performed exactly for the underlying canonical ensemble consisting of a given number of particles. We discuss the viability of the partition temperature in this case. Possible implications of the obtained results regarding the observed Tsallis distribution in transverse momentum spectra in high-energy collisions are also addressed.

Keywords: partition temperature; Darwin–Fowler; saddle point approximation; jet; high-energy collisions

1. Introduction

In high-energy hadronic collisions, the outgoing particle that possesses the same quantum numbers as the incoming one is known as the leading particle, whose identification allows us to obtain additional details about the kinematics of the scattering process. For high-energy collisions [1–3], it was proposed that for the semi-inclusive scattering processes [4–7], the single-particle distribution for (all of the remaining) nonleading particles can be derived from the joint exclusive probability distribution [8]. Specifically, the latter is essentially a micro-canonical ensemble consisting of n particles under the relevant conservation laws, which reads

$$\mathcal{P} = \prod_{l=1}^{n} \frac{d^3 \mathbf{p}_l}{E_l} g(\mathbf{p}_1, \mathbf{p}_2, \cdots, \mathbf{p}_n) \delta \left[\sum_{i=1}^{n} p_{Li} - P_L \right] \delta^2 \left[\sum_{j=1}^{n} \mathbf{p}_{Tj} - \mathbf{P}_T \right] \delta \left[\sum_{k=1}^{n} E_k - W \right], \qquad (1)$$

where W, P_L, and $\mathbf{P}_T$ are the total energy and longitudinal and transversal momenta of the N-particle system in the center-of-mass frame and $g(\mathbf{p}_1, \cdots, \mathbf{p}_n)$ refers to some additional constraint of the phase space, whose form in this study will be made explicit below in

Equation (14). To focus on the single-particle spectrum, one integrates out the degrees of freedom associated with the remaining $n-1$ particles to find

$$\frac{d^3\bar{n}}{dyd\mathbf{p}_T} = \int \prod_{l=2}^{n} \frac{d^3\mathbf{p}_l}{E_l} g(\mathbf{p}, \mathbf{p}_2, \cdots, \mathbf{p}_n) \delta\left[\sum_{i=2}^{n} p_{Li} + p_L - P_L\right] \delta^2\left[\sum_{j=2}^{n} \mathbf{p}_{Tj} + \mathbf{p}_T - \mathbf{P}_T\right] \delta\left[\sum_{k=2}^{n} E_k + E - W\right], \qquad (2)$$

One manifestly arrives at a canonical ensemble

$$\frac{d^3\bar{n}}{dyd\mathbf{p}_T} \propto \exp\left(-\frac{E}{T_p}\right), \qquad (3)$$

for a single particle with longitudinal and transverse momenta p_L and $\mathbf{p}_T$, rapidity $y = \ln\frac{E+p_L}{E-p_L}$, and energy E, where T_p effectively plays the role of temperature and is referred to as partition temperature [9]. Such an endeavor was explicitly carried out in [8], which primarily employs the following assumptions and approximations. (1) The momentum conservation in the transverse direction is largely ignored. (2) A specific form of the density function $f(y, \mathbf{p}_T)$ is assumed, c.f. Equation (6). (3) It was argued that the integral in $\eta = \sqrt{(\beta+s)^2 - t^2}$ (where some relevant variables are defined in Equations (7)) is dominated by the region $\eta \to 0$, and thus an approximate form is used. (4) The saddle approximation is employed for the integral in $\zeta = \text{arctanh}\left(\frac{t}{\beta+s}\right)$. Subsequently, the obtained analytic results on the partition temperatures were compared against those obtained by fitting to the experimental data for $p\bar{p}$ collisions at 540 GeV [10]. By adopting the parameters extracted from the data, excellent agreement was achieved, where, for the most part, the discrepancies were less than 5%.

In principle, the Boltzmann–Gibbs characteristic of the above results can be understood [10,11] in terms of the Darwin–Fowler framework [9]. In this regard, the notion of partition temperature T_p emerges from a contour integration in terms of a *selector variable* [12], which is utilized to enforce the relevant conservation laws. Specifically, the common parameter between different assemblies resulting from such an approach bears a resemblance to the temperature and is referred to in the literature as partition temperature. It is noted that the feasibility of the Darwin–Fowler formalism largely resides in the validity of the saddle point method, which is often employed to approximate the contour integration. In particular, the partition function is essentially governed by the location of the saddle point. Even though the partition is obtained without referring to the thermodynamic equilibrium, its link to other thermodynamic quantities such as entropy has been elaborated [13]. In this approach, the saddle point corresponds to a strong maximum on the contour in question, which is true when the thermodynamic limit is attained. However, if the relevant degrees of freedom are not significant, numerical calculations indicate that further caution might be taken [14]. To be more precise, the derivation based on the approximation and, subsequently, the notion of partition temperature might cease to be valid. Calculations need to be performed to validate the partition temperature for the specific scenario in question. As discussed below, the feasibility of partition temperature plays an essential role in the observed Tsallis distribution; therefore, the resultant particle distribution at small multiplicities is physically pertinent.

The calculations [8] carried out by explicit phase-space integration also employed the saddle point method. It was found that the divergence becomes more significant for smaller multiplicities. When scrutinizing the results more closely, it was pointed out [8] that the results did not correctly reproduce the dependence of average transverse momentum on the event multiplicity, despite the apparent success of reproducing the partition temperature. Moreover, the deviation increases further if one redefines the total energy using the experimental data on transverse momentum. This, in turn, leads to some degree of speculation about whether the notion of partition temperature is indeed valid in such a context, such as $\bar{p}p$ collisions, where the overall multiplicity is not significant.

For a wide range of pp, $p\bar{p}$, AA, and e^+e^- collisions, the transverse-momentum spectrum for the intermediate and high momentum range ($p_T \gtrsim 3$ GeV) cannot be described using a Boltzmann–Gibbs distribution. However, the resulting Tsallis distribution can still be understood in the framework of superstatistics. Specifically, since the system is not homogeneous, one may obtain the Tsallis distribution by assuming that the observed spectrum corresponds to an ensemble average of subsystems where either the temperature [15] or multiplicity [16,17] fluctuates. It can be shown that an additional parameter, q, associated with the Tsallis-like distribution, measures the strength of fluctuations in either temperature or multiplicity. In this context, the notion of partition function continues to play a significant role in these studies.

The present study is motivated by the above discussions. We aim at a scenario where the contour integral can be performed precisely to steer clear of the uncertainty related to the saddle point approximation when the multiplicity is small. To this end, we elaborate on the case of massless particles where the phase-space integration can be evaluated without saddle point approximation. In this regard, the obtained result presents another explicit example where the concept of partition temperature is valid.

The remainder of the paper is organized as follows. In the following section, we give a detailed account of the general form of the phase-space integration that gives rise to the one-particle distribution from the microcanonical ensemble, essentially based on results obtained in Ref. [8]. In Section 3, the specific contour integration is carried out precisely, and the results are presented. We conduct numerical analysis in Section 4 and discuss the viability of the extracted partition temperatures. Further discussions and concluding remarks are given in the last section.

2. Phase-Space Integration of the One-Particle Momentum Distribution

We start by considering a system of N particles with a total energy of W, a momentum of $\mathbf{P}$, and a subsequently total invariant mass $M = \sqrt{W^2 - \mathbf{P}^2}$. The particle's mass is denoted by m, which will be taken to be zero.

Following [8], we divide the phase space into N small intervals whose occupation numbers will be denoted as n_ℓ with $\ell = 1, 2, \cdots, N$. The probability of finding a microscopic distribution $\{n_\ell\} \equiv \{n_1, \cdots, n_N\}$, Equation (1), takes the form

$$\mathcal{P}(\{n_\ell\}) = \frac{n!}{n_1! \cdots n_N!} q_1^{n_1} \cdots q_N^{n_N} \delta_{\left(n, \sum_{\ell=1}^{N} n_\ell\right)} \delta\left[\sum_{i=1}^{N} n_i p_{Li} - P_L\right] \delta^2\left[\sum_{j=1}^{N} n_j \mathbf{p}_{Tj} - \mathbf{P}_T\right] \delta\left[\sum_{k=1}^{N} n_k E_k - W\right], \tag{4}$$

where q_ℓ stands for the probability of finding a particle in the phase space interval ℓ. Apparently, q_ℓ is proportional to the volume of the phase space $dV = dy d\mathbf{p}_T$, so that $q_\ell = f(y_\ell, \mathbf{p}_{T\ell}) dy d\mathbf{p}_T$, where the probability density function $f(y, \mathbf{p}_T)$ is normalized

$$\sum_{\ell=1}^{N} q_\ell = 1 \rightarrow \lim_{N \to \infty} \sum_{\ell=1}^{N} q_\ell = \int f(y, \mathbf{p}_T) dy d\mathbf{p}_T = 1. \tag{5}$$

One takes $f(y, \mathbf{p}_T) = 1$ if the occupation probability is simply proportional to the volume of the phase space.

Using the probability given by Equation (4), the single particle momentum Equation (2) distribution reads

$$\left.\frac{d^3\bar{n}}{dy d\mathbf{p}_T}\right|_{n,W,P} \equiv \langle n_k \rangle = \frac{\sum_{\{n_\ell\}} P(\{n_\ell\}) n_k}{\sum_{\{n_\ell\}} P(\{n_\ell\})} \equiv \frac{A}{B}. \tag{6}$$

We note that both Equations (4) and (6) have explicitly taken into account the conservation of the total number of particles, momentum, and energy.

To deal with the conservation of energy and longitudinal momentum, we introduce two Laplace transforms in the variables s and t and rewrite these quantities in terms of trans-

verse momentum and rapidity, namely, $E = \sqrt{\mathbf{p}_T^2 + m^2}\cosh y$ and $p_L = \sqrt{\mathbf{p}_T^2 + m^2}\sinh y$. Specifically, we have

$$\delta\left[\sum_{k=1}^{N} n_k E_k - W\right] = \int_{\epsilon_0 - i\infty}^{\epsilon_0 + i\infty} ds\exp\left[\left(W - \sum_{k=1}^{N} n_k E_k\right)s\right] = \int_{\epsilon_0 - i\infty}^{\epsilon_0 + i\infty} ds e^{Ws}\prod_{k=1}^{N}\left[e^{-E_k s}\right]^{n_k}$$

$$\delta\left[\sum_{i=1}^{N} n_i p_{Li} - P_L\right] = \int_{\epsilon_1 - i\infty}^{\epsilon_1 + i\infty} dt\exp\left[-\left(P_L - \sum_{i=1}^{N} n_i p_{Ti}\right)t\right] = \int_{\epsilon_1 - i\infty}^{\epsilon_1 + i\infty} dt e^{-P_L t}\prod_{i=1}^{N}\left[e^{p_{Li} t}\right]^{n_i}, \tag{7}$$

where $\epsilon_0 = \Re s > \Re t = \epsilon_1 \geq 0$, so the integrals are convergent. The conservation law for the transversal momentum can be treated similarly by introducing the Fourier transform of a two-dimensional delta function

$$\delta^2\left[\sum_{j=1}^{n}\mathbf{p}_{Tj} - \mathbf{P}_T\right] = \int d\mathbf{u}_T\exp\left[-i\left(\mathbf{P}_T - \sum_{j=1}^{N} n_j\mathbf{p}_{Tj}\right)\cdot\mathbf{u}_T\right] = \int d\mathbf{u}_T e^{-i\mathbf{P}_T\cdot\mathbf{u}_T}\prod_{j=1}^{N}\left[e^{i\mathbf{p}_{Tj}\cdot\mathbf{u}_T}\right]^{n_j}. \tag{8}$$

The Kronecker delta responsible for particle number conservation can be dealt with by noticing the relation

$$\delta_{\left(n,\sum_{\ell=1}^{N} n_\ell\right)} = \int_0^{2\pi} dv\exp\left[-i\left(n - \sum_{\ell=1}^{N} n_\ell\right)v\right]. \tag{9}$$

By plugging Equations (7)–(9) into the numerator of Equation (6) and picking out the terms related to the occupation numbers, we have

$$\left.\frac{d^3\bar{n}}{dy d\mathbf{p}_T}\right|_{n,W,P} \equiv \langle n_k\rangle \simeq n f(y,\mathbf{p}_T) dy d\mathbf{p}_T\frac{C}{D}, \tag{10}$$

where

$$C = \int_{\epsilon_0 - i\infty}^{\epsilon_0 + i\infty} ds\int_{\epsilon_1 - i\infty}^{\epsilon_1 + i\infty} dt[F(s,t)]^{n-1}\times\exp[(W - p_T\cosh y)s - (P_L - p_T\sinh y)t], \tag{11}$$

$$D = \int_{\epsilon_0 - i\infty}^{\epsilon_0 + i\infty} ds\int_{\epsilon_1 - i\infty}^{\epsilon_1 + i\infty} dt[F(s,t)]^{n}\exp[Ws - P_L t], \tag{12}$$

and

$$F(s,t,\mathbf{u}_T) = dy d\mathbf{p}_T f(y,\mathbf{p}_T)\exp[-p_T(s\cosh y - t\sinh y) + i\mathbf{p}_T\cdot\mathbf{u}_T]. \tag{13}$$

We relegate the details of the derivations of Equations (11) and (12) to Appendix A.

It is noted that the integrations in s and t given by Equations (A9), (A10), (11) and (12) still pose a challenge for most scenarios. For most cases, the approximation method is indispensable. In particular, the saddle point approximation was employed for the ansatz in [8].

3. The Contour Integration

In this section, we elaborate on a simplified scenario that remains physically relevant while avoiding the need for any approximations. Specifically, we constrain the emission of massless particles entirely to the longitudinal direction, with the probability density function taking the form

$$f(p) = \alpha e^{-\beta|p|}, \tag{14}$$

where $\beta > 0$ and $\alpha = \beta/2$ serve as the normalization constant. Notably, the parameter β should not be construed as a "temperature". As it turns out, the specific form of Equation (14) simplifies the integrations, and its role is primarily technical to ensure the convergence of the integrations. Furthermore, as discussed below, the *pure* phase space integral can be readily recovered by taking the limit $\beta \to 0_+$ at the end of the calculations.

Subsequently, $F(s, t)$, defined by Equation (A4) has the following form:

$$
\begin{aligned}
F(s, t) &= \frac{\beta}{2} \int_{-\infty}^{\infty} \exp[-(\beta + s)|p| + pt], \\
&= \frac{\beta}{2} \left[\int_{-\infty}^{0} \exp[(t + \beta + s)p] + \int_{0}^{\infty} \exp[-(\beta + s - t)p] \right], \\
&= \frac{\beta}{2} \left[\frac{1}{t + \beta + s} + \frac{1}{t - \beta - s} \right], \\
&= \frac{\beta(\beta + s)}{(\beta + s)^2 - t^2},
\end{aligned}
\tag{15}
$$

where one requires $\Re s > \Re t \geq 0$ so that the integrals are well-defined. We note the simplification brought to Equation (A4) in this case, which also benefits from the form given by Equation (14). On the contrary, the exponential cannot be simplified for massive particles, which eventually leads to further change in variables and the saddle approximation.

Now, we proceed to evaluate C and D defined by Equations (A9) and (A10). For the denominator, we have

$$
\begin{aligned}
D &= \int_{\epsilon_0 - i\infty}^{\epsilon_0 + i\infty} ds \int_{\epsilon_1 - i\infty}^{\epsilon_1 + i\infty} dt \left[\frac{\beta(\beta + s)}{(\beta + s)^2 - t^2} \right]^n \exp(Ms) \\
&= \beta^n \int_{\epsilon_0 - i\infty}^{\epsilon_0 + i\infty} ds (\beta + s)^n \exp(Ms) \int_{\epsilon_1 - i\infty}^{\epsilon_1 + i\infty} dt\, G(t).
\end{aligned}
\tag{16}
$$

where

$$
G(t) = \left[\frac{1}{(\beta + s)^2 - t^2} \right]^n,
\tag{17}
$$

and one has utilized the relation $W = M$ and $P = 0$ in the center of mass frame of the jet.

The integral in t can be performed using the residue theorem by completing the contour in the counterclockwise direction on an infinite semi-circle. The analytic function $G(t)$ has two n-th order poles. By picking up the relevant one on the l.h.s. of the imaginary axis $t_0 = -(\beta + s)$, one finds

$$
\begin{aligned}
D &= \beta^n \int_{\epsilon_0 - i\infty}^{\epsilon_0 + i\infty} ds (\beta + s)^n \exp(Ms) \int_{\epsilon_1 - i\infty}^{\epsilon_1 + i\infty} dt\, G(t) \\
&= \beta^n \int_{\epsilon_0 - i\infty}^{\epsilon_0 + i\infty} ds (\beta + s)^n \exp(Ms) \oint_C dt\, G(t) \\
&= \beta^n \int_{\epsilon_0 - i\infty}^{\epsilon_0 + i\infty} ds (\beta + s)^n \exp(Ms) 2\pi i \operatorname{Res}(G, t_0) \\
&= \frac{2\pi i \beta^n (2n - 2)!}{2^{2n-1}[(n-1)!]^2} \int_{\epsilon_0 - i\infty}^{\epsilon_0 + i\infty} ds\, H(s),
\end{aligned}
\tag{18}
$$

where

$$
H(s) = \frac{e^{Ms}}{(s + \beta)^{n-1}},
\tag{19}
$$

as it is straightforward to find

$$
\begin{aligned}
\mathrm{Res}(G, t_0) &= \frac{1}{(n-1)!} \lim_{t \to t_0} \frac{d^{n-1}}{dt^{n-1}} \left((t-t_0)^n G(t) \right) \\
&= \frac{1}{(n-1)!} \lim_{t \to t_0} \frac{d^{n-1}}{dt^{n-1}} \frac{(-1)^n}{(t+t_0)^n} \\
&= \frac{(-1)^n}{(n-1)!} \frac{(-n)(-n-1)\cdots(-2n+2)}{(2t_0)^{2n-1}} \\
&= \frac{(2n-2)!}{[(n-1)!]^2 [2(\beta+s)]^{2n-1}}.
\end{aligned}
\tag{20}
$$

The last integral of Equation (19) can again be performed using residue theorem by using Jordan's lemma and enclosing the contour in the counterclockwise direction on an infinite semi-circle. By picking out the contribution from a residual on the negative real axis $s = -\beta$, we have

$$
\begin{aligned}
\oint_C H(s)\,ds &= 2\pi i \mathrm{Res}(H, -\beta) \\
&= \frac{2\pi i}{(n-2)!} \lim_{s \to -\beta} \frac{d^{n-2}}{ds^{n-2}} \left((s+\beta)^{n-2} H(s) \right) \\
&= \frac{2\pi i}{(n-2)!} \lim_{s \to -\beta} \frac{d^{n-2}}{ds^{n-2}} e^{Ms} \\
&= \frac{2\pi i M^{n-2}}{(n-2)!} e^{-\beta M}.
\end{aligned}
\tag{21}
$$

Therefore, one obtains

$$
D = \frac{-\pi^2 (2n-2)! \beta^2 (\beta M)^{n-2}}{2^{2n-3}[(n-1)!]^2 (n-2)!} e^{-\beta M}.
\tag{22}
$$

The calculation of Equation (A9) can be carried out in a similar fashion, and we have

$$
\begin{aligned}
C &= \int_{\epsilon_0 - i\infty}^{\epsilon_0 + i\infty} ds \int_{\epsilon_1 - i\infty}^{\epsilon_1 + i\infty} dt \left[\frac{\beta(\beta+s)}{(\beta+s)^2 - t^2} \right]^{n-1} \exp[(M - |p|)s + pt] \\
&= \beta^{n-1} \int_{\epsilon_0 - i\infty}^{\epsilon_0 + i\infty} ds\, (\beta+s)^{n-1} \exp[(M - |p|)s] \int_{\epsilon_1 - i\infty}^{\epsilon_1 + i\infty} dt \frac{e^{pt}}{[(\beta+s)^2 - t^2]^{n-1}} \\
&= 2\pi i \beta^{n-1} \sum_{r=0}^{n-2} \frac{(n+r-2)!}{r!(n-r-2)!} \frac{p^{n-2-r} e^{-p\beta}}{2^{n+r-1}} \int_{\epsilon_0 - i\infty}^{\epsilon_0 + i\infty} ds \frac{\exp[(M - |p| - p)s]}{(\beta+s)^r} \\
&= (2\pi i)^2 \beta^{n-1} \sum_{r=0}^{n-2} \frac{(n+r-2)!}{r!(n-r-2)!} \frac{p^{n-2-r} e^{-p\beta}}{2^{n+r-1}} \frac{(M - |p| - p)^{r-1}}{(r-1)!} e^{-\beta(M - |p| - p)} \\
&= -4\pi^2 \beta^{n-1} e^{-\beta(M - |p|)} \sum_{r=0}^{n-2} \frac{(n+r-2)!}{2^{n+r-1} r! (r-1)! (n-r-2)!} p^{n-2-r} (M - |p| - p)^{r-1}.
\end{aligned}
\tag{23}
$$

In the above calculations, the integral in t can be carried out for

$$
G = G(t) = \frac{(-1)^{n-1} e^{pt}}{[t - (\beta+s)]^{n-1} [t + (\beta+s)]^{n-1}},
\tag{24}
$$

using Jordan's lemma. Both residues at $t_{1,2} = \pm(\beta+s)$ are relevant, as one must choose the counterclockwise (clockwise) contour when $p > 0$ ($p < 0$). Specifically, for $p > 0$, we have

$$
\begin{aligned}
\mathrm{Res}(G, t_2) &= \frac{(-1)^{n-2}}{(n-2)!} \lim_{t \to t_2} \left[\frac{d^{n-2}}{dt^{n-2}} \frac{e^{pt}}{(t-t_1)^{n-1}} \right] \\
&= \frac{(-1)^{n-2}}{(n-2)!} \lim_{t \to t_2} \sum_{r=0}^{n-2} \binom{n-2}{r} \left[\frac{d^{n-2-r}}{dt^{n-2-r}} e^{pt} \right] \left[\frac{d^r}{dt^r} \frac{1}{(t-t_1)^{n-1}} \right] \\
&= \frac{(-1)^{n-2}}{(n-2)!} \lim_{t \to t_2} \sum_{r=0}^{n-2} \binom{n-2}{r} \left[p^{n-2-r} e^{pt} \right] \frac{(-1)^r (n-1)n \cdots (n+r-2)}{(t-t_1)^{n+r-1}} \\
&= \sum_{r=0}^{n-2} \binom{n-2}{r} \frac{n \cdots (n+r-2) p^{n-2-r} e^{-p(\beta+s)}}{2^{n+r-1}(\beta+s)^{n+r-1}} \\
&= \sum_{r=0}^{n-2} \frac{(n+r-2)!}{r!(n-r-2)!} \frac{p^{n-2-r} e^{-p(\beta+s)}}{2^{n+r-1}(\beta+s)^{n+r-1}}.
\end{aligned}
\tag{25}
$$

The integral in s, the exponential $(M - |p| - p) > 0$, dictates the use of Jordan's lemma, and the residue of

$$
H(s) = \frac{e^{(M-|p|-p)s}}{(\beta+s)^r}
\tag{26}
$$

at $s = -\beta$ is found to be

$$
\begin{aligned}
\mathrm{Res}(H, -\beta) &= \frac{1}{(r-1)!} \lim_{s \to -\beta} \left[\frac{d^{r-1}}{ds^{r-1}} e^{(M-|p|-p)s} \right] \\
&= \frac{(M-|p|-p)^{r-1}}{(r-1)!} e^{-\beta(M-|p|-p)}.
\end{aligned}
\tag{27}
$$

We note that when $p < 0$, the integral in t leads to a factor with exponential dependence of $e^{p(\beta+s)}$. A similar expression is obtained after performing the integration in s.

Putting the pieces together, we have

$$
\left. \frac{d\bar{n}}{dp} \right|_{n,W,P} \equiv \langle n_k \rangle = n f(p) dp \frac{C}{D} \propto \sum_{r=0}^{n-2} \frac{(n+r-2)!}{2^{n+r-1} r!(r-1)!(n-r-2)!} \times p^{n-r-2}(M-|p|-p)^{r-1},
\tag{28}
$$

where it is noteworthy that the exponential term $\exp[-\beta|p|]$ cancels out identically. In other words, the obtained one-particle distribution does not depend on the specific value of β, as taking the limit $\beta \to 0_+$ yields no changes to the resultant expression. Additionally, based on the form of Equation (28), it is unclear whether the resultant one-particle distribution can be characterized by any sort of partition temperature.

4. The Feasibility of Partition Temperature

The one-particle distribution function obtained in the last section, Equation (28), possesses a rather tedious form consisting of a summation of polynomials in p. In this section, we numerically evaluate the resulting distribution function and use a non-linear fit to extract the associated partition temperature.

The corresponding numerical results are shown in Figures 1 and 2 and Table 1. As the results mainly aim to demonstrate the feasibility of the effective temperature, the assumed values do not refer to any specific scenario, and natural units are used. The calculations are carried out for a given average $\bar{p}$ so that the total mass reads $M = W = n\bar{p}$. The summations in Equation (28) are carried out numerically and sampled at $N_{\text{sample}} = 50$ points evenly distributed on the interval $p \in (0, 2\bar{p})$. The calculations are for different multiplicities $n = 5, 10, 50$, and 100. Also, without loss of generality, we take $\bar{p} = 10$. We have confirmed that the qualitative conclusion drawn below remains unchanged, independent of this specific choice.

In order to assess the validity of partition temperature, a nonlinear fit is carried out regarding the above range and depicted on top of the numerical results. By using the *Mathematica* build-in module NonlinearModelFit[], the resultant one-particle distribution function is fit to an exponential form $y = A \exp(-p/T_p)$. The fit is performed under the assumption that the numerical values y_i ($i = 1, \cdots, 50$) are independent and normally distributed with a mean of $\hat{y}_i$ and a common standard deviation. The results are presented in Figure 1, where black curves show the nonlinear fits, and the numerical distribution functions are shown in solid red symbols. It is somewhat surprising that even for $n = 5$, the one-particle distribution function agrees reasonably well with the notion of partition temperature. As the multiplicity increases, the agreement further improves, as shown in the left panel of Figure 2.
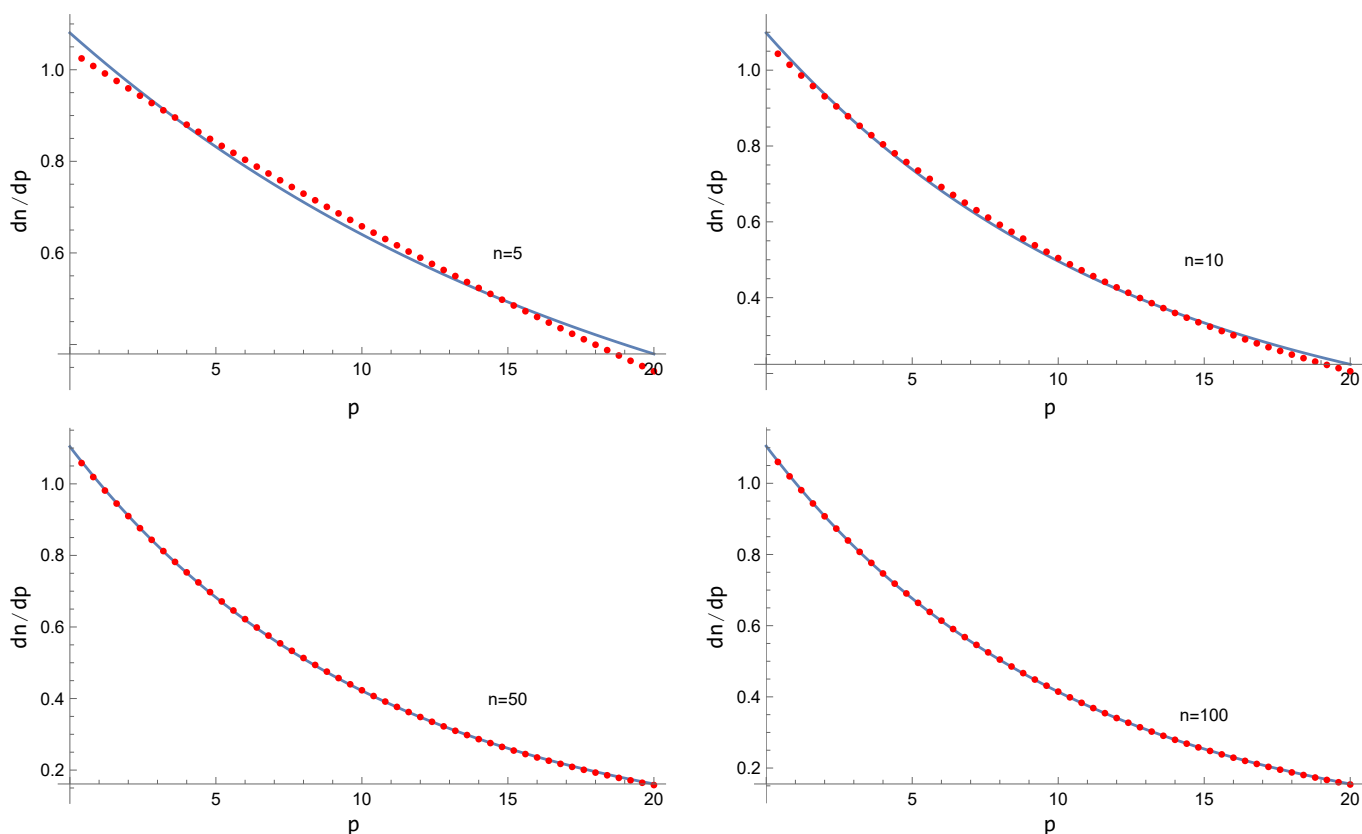
Figure 1. Left: The numerical fits shown in Figure 1 but presented in the logarithmic scale. From the top to bottom, the curves correspond to the multiplicities $n = 5, 10, 50$, and 100, respectively. Right: The extracted partition temperature $1/T_p$ as a function of the multiplicity n, where the red dashed curve is obtained by a third-order spline fit.

More specific values of the extracted partition temperatures and the goodness of the fits are shown in Table 1. As a measure of the fit's quality, the standard error is defined as the standard deviation divided by the square root of the number of samples. Furthermore, the p-values are also evaluated, which give the probabilities, under the null hypothesis, of obtaining a result equal to or more extreme than the sampled points. The smallness of both quantities indicates the partition temperature's feasibility; moreover, the fit becomes more reliable at large multiplicities. For small multiplicity, however, the extracted value of partition temperature is not a constant. This is understood as an indication that the quantity is irrelevant to thermodynamic equilibrium. As the multiplicity increases, one observes that the partition temperature converges, as indicated by the right panel of Figure 2. It is interesting to point out that the effective temperature extracted numerically indicates that $T_p \to \bar{p}$ at the limit $n \to \infty$. Nonetheless, it is also noted that the notion of partition function breaks down for the high-momentum region.

Table 1. The extracted partition temperatures, the corresponding standard errors, and *p*-values for different multiplicities *n*. The quality of the fit improves as the multiplicity increases.

n	5	10	30	40	50	100
$1/T_p$	0.0523	0.0794	0.0936	0.0952	0.0962	0.0981
standard error	0.0006	0.0005	0.0002	0.0001	0.0001	0.00005
p-value	1.2×10^{-51}	9.5×10^{-67}	3.0×10^{-91}	1.9×10^{-97}	3.2×10^{-102}	6.5×10^{-117}
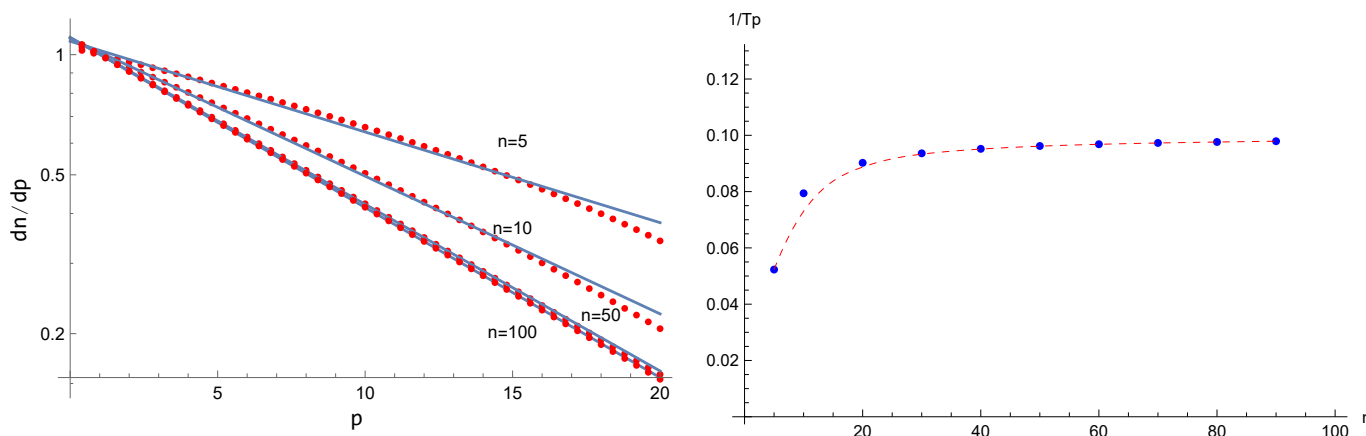
Figure 2. The numerical fits shown in Figure 1 but presented in the logarithmic scale (**left**) and the extracted partition temperature $1/T_p$ as a function of the multiplicity *n* (**right**), where the red dashed curve is obtained using a third-order spline fit.

5. Further Discussions and Concluding Remarks

The notion of partition temperature with the Darwin–Fowler approach is widely known, and the result is exact for simple scenarios. As a result, it is often accepted and borrowed in different contexts without further scrutinization. Nonetheless, for complex systems, the validity of the partition temperature resides on some approximations, such as the saddle point method, and subsequently, further caution should be taken. The present study explores a scenario pertinent to particle emission in relativistic high-energy collisions, which possesses an analytic closed form for the resulting one-particle distribution. It is observed that even the analytic result does not imply the existence of an effective temperature, and the distribution converges rapidly to an exponential form for particles with low and intermediate momenta. Nonetheless, it is noted that the notion of partition temperature breaks down for the high-momentum region. We also note that the general scenario with massive particles and the momentum in the transverse direction is essential. While it is mainly handicapped, as an analytic closed-form solution is often not accessible, it might be feasible to carry out numerical studies.

In the transverse direction, experimental data from ATLAS [18], ALICE [19], and CMS [20–22] have shown that the transverse-momentum spectra of hadrons for various collision systems and at various collision energies are very well described by a Tsallis distribution [23–25]. As a generalization of standard Boltzmann–Gibbs statistics, the Tsallis distribution is derived by maximizing the Tsallis entropy under appropriate constraints. From the side of data analysis, it properly accounts for the observed slowly decreasing tails obeying the power law. Besides the phenomenological formula proposed by Hagedorn [26], a natural recipe is to employ the relativistic hard-scattering model in perturbative QCD. It was intriguing to observe that the experimental hadron transverse differential cross section appears to differ from what one expects from the intuitive partonic collision viewpoint [27–29]. To be specific, in the context of the quark model, the high-p_T differential cross section in a $2 \rightarrow 2$ exclusive process can be inferred from a scaling law [27–29], leading

to a different power index from the data. This fact was subsequently interpreted in terms of the counting rule of the parton-meson degrees of freedom [30–33].

The present study, however, concerns an alternative line of thought that does not directly involve the underlying dynamics. We primarily focus on the phase space distribution regarding the kinematic variables by scrutinizing the partition and constraints of the phase space from a statistical viewpoint. Specifically, statistics turns out to play an intriguing role in the relevant analyses [15–17,34–38], where the notion of local partition temperature is a pertinent concept. For instance, since the system is not homogeneous, it can be argued that the partition temperature fluctuates. Wilk and Wlodarczyk showed that an additional parameter, q, which measures the strength of fluctuations in temperature, readily gives rise to the desired q-exponential distribution [15], furnishing a plausible explanation of the data. Alternatively, if the momentum distribution in an event with fixed multiplicity is featured by a partition function, and the multiplicity fluctuates according to a Gamma distribution, the average momentum distribution also obeys a Tsallis-like form [16,17]. Again, in this case, the variance of the multiplicity distribution is associated with the parameters of the Tsallis-type distribution. It is thus understood that the apparent validity of such a line of thought indicates that the resulting Tsallis-like distribution is not entirely a manifestation of the underlying dynamics, namely, the QCD.

It is worth noting that the above two approaches can be viewed consistently under appropriate circumstances. As pointed out by Wong and Wilk [39], if one considers the showering and hadronization processes of the parton jets on top of the multiple hard scattering of partons, the experimentally observed Tsallis-type distributions can be reasonably explained. On the one hand, by analyzing the experimental results of jet transverse differential cross sections with the relativistic hard-scattering model, it is concluded that the jet production can be approximately described by the relativistic hard-scattering model that appropriately takes into account the effects of multiple scattering and partition thicknesses. On the other hand, the showering and hadronization processes further push the power index to a more significant value observed experimentally. By comparing this picture with the discussions on the statistical side, the latter corresponds to the collinear hadron emission from a given jet. Employing the phase-space integral, the distribution is then estimated at the center-of-mass frame of individual jets, which typically is not of significant relative momentum. Although the finite size of the underlying phase space implies that the distribution will not have an extensive tail at a small momentum, it becomes an exponential function consistent with those of phenomenological models. Moreover, by convoluting the above two ingredients, it was argued that the resulting distribution is essentially the Tsallis type [16,17]. In this regard, the present study is qualitative, with the primary goal of demonstrating the feasibility of effective temperature when the multiplicity is small. It is worth conducting further analyses regarding a quantitative comparison with the observed Tsallis distribution in the data.

Author Contributions: Conceptualization and methodology: W.-L.Q., Y.H. and T.K. All authors have involved in investigation and writing. All authors have read and agreed to the published version of the manuscript.

Data Availability Statement: The numerical results can be readily generated by the method discussed in the manuscript.

Conflicts of Interest: The authors declare no conflict of interest.

Appendix A. The Derivations of the Formuale for One-Particle Distribution Function

In this appendix, we give an account of Equations (10)–(12) utilized in the main text.

By plugging Equations (7)–(9) into the numerator of Equation (6) and picking out the terms related to the occupation numbers, we have

$$
\sum_{\{n_\ell\}} n! \int_0^{2\pi} dv \exp\left[-i\left(n - \sum_{\ell=1}^N n_\ell\right)v\right] \left[\frac{\left(q_1 e^{-(E_1 s - p_{L1} t + i\mathbf{p}_{T1}\cdot\mathbf{u}_T)}\right)^{n_1}}{n_1!}\right] \cdots \left[\frac{\left(q_N e^{-(E_N s - p_{LN} t + i\mathbf{p}_{TN}\cdot\mathbf{u}_T)}\right)^{n_N}}{n_N!}\right]
$$

$$
= \sum_{\{n_\ell\}} n! \int_0^{2\pi} dv\, e^{-inv} \exp\left[\sum_{\ell=1}^N ivn_\ell\right] \left[\frac{\left(q_1 e^{-(E_1 s - p_{L1} t + i\mathbf{p}_{T1}\cdot\mathbf{u}_T)}\right)^{n_1}}{n_1!}\right] \cdots \left[\frac{\left(q_N e^{-(E_N s - p_{LN} t + i\mathbf{p}_{TN}\cdot\mathbf{u}_T)}\right)^{n_N}}{n_N!}\right]
$$

$$
= \sum_{\{n_\ell\}} n! \int_0^{2\pi} dv\, e^{-inv} \left[\frac{\left(q_1 e^{-(E_1 s - p_{L1} t + i\mathbf{p}_{T1}\cdot\mathbf{u}_T)}\right)^{n_1}}{n_1!}\right] \cdots \left[\frac{\left(q_N e^{-(E_N s - p_{LN} t + i\mathbf{p}_{TN}\cdot\mathbf{u}_T)}\right)^{n_N}}{n_N!}\right] \prod_{\ell=1}^N \left[e^{iv}\right]^{n_\ell} \tag{A1}
$$

$$
= \sum_{\{n_\ell\}} n! \int_0^{2\pi} dv\, e^{-inv} \prod_{\ell=1}^N \frac{\left[q_\ell e^{-(E_\ell s - p_{L\ell} t)} e^{iv}\right]^{n_\ell}}{n_\ell!}
$$

$$
= n! \int_0^{2\pi} dv\, e^{-inv} \prod_{\ell=1}^N \sum_{n_\ell=1}^{\infty} \frac{\left[q_\ell e^{-(E_\ell s - p_{L\ell} t + i\mathbf{p}_{T\ell}\cdot\mathbf{u}_T)} e^{iv}\right]^{n_\ell}}{n_\ell!}
$$

$$
= n! \int_0^{2\pi} dv\, e^{-inv} \prod_{\ell=1}^N \exp\left[q_\ell e^{-(E_\ell s - p_{L\ell} t + i\mathbf{p}_{T\ell}\cdot\mathbf{u}_T)} e^{iv}\right],
$$

where the remaining integral in v will still turn out to be manageable. A similar derivation can be carried out for the denominator of Equation (6).

To proceed, we note that the part involving the product $\prod_{\ell=1}^N$ between phase space intervals can be concluded as follows

$$
\prod_{\ell=1}^N \exp\left[q_\ell e^{-(E_\ell s - p_{L\ell} t + i\mathbf{p}_{T\ell}\cdot\mathbf{u}_T)} e^{iv}\right] = \exp\left[\sum_{\ell=1}^N q_\ell e^{-(E_\ell s - p_{L\ell} t + i\mathbf{p}_{T\ell}\cdot\mathbf{u}_T)} e^{iv}\right], \tag{A2}
$$

and therefore

$$
\lim_{N\to\infty} \prod_{\ell=1}^N \exp\left[q_\ell e^{-(E_\ell s - p_{L\ell} t + i\mathbf{p}_{T\ell}\cdot\mathbf{u}_T)} e^{iv}\right] = \exp\left[F(s,t,\mathbf{u}_T) e^{iv}\right], \tag{A3}
$$

where

$$
F(s,t,\mathbf{u}_T) \equiv \lim_{N\to\infty} \sum_{\ell=1}^N q_\ell e^{-(E_\ell s - p_{L\ell} t + i\mathbf{p}_{T\ell}\cdot\mathbf{u}_T)} = dy\, d\mathbf{p}_T\, f(y,\mathbf{p}_T) \exp\left[-\sqrt{\mathbf{p}_T^2 + m^2}(s\cosh y - t\sinh y) + i\mathbf{p}_T\cdot\mathbf{u}_T\right]. \tag{A4}
$$

The resulting contribution that involves the integral in v can be dealt with analytically. For the numerator, it possesses the following form:

$$
\int_0^{2\pi} dv \exp[-inv] \exp\left[F(s,t,\mathbf{u}_T) e^{iv}\right]
$$

$$
= \int_0^{2\pi} dv \exp[-inv] \sum_{l=0}^{\infty} \frac{F(s,t,\mathbf{u}_T)^l e^{ilv}}{l!}
$$

$$
= \sum_{l=0}^{\infty} \frac{1}{l!} \int_0^{2\pi} dv \exp[-i(n-l)v] F(s,t,\mathbf{u}_T)^l \tag{A5}
$$

$$
= \sum_{l=0}^{\infty} \frac{F(s,t,\mathbf{u}_T)^l}{l!} \delta_{n,l}
$$

$$
= \frac{F(s,t,\mathbf{u}_T)^n}{n!}.
$$

By putting the above pieces together, one simplifies Equation (6) into the following forms [8]:

$$
\begin{aligned}
A &= \frac{-n}{(2\pi)^4} f(y, \mathbf{p}_T) dy d\mathbf{p}_T \int_{\epsilon_0 - i\infty}^{\epsilon_0 + i\infty} ds \int_{\epsilon_1 - i\infty}^{\epsilon_1 + i\infty} dt \int du_T [F(s, t, u_T)]^{n-1} \\
&\times \exp\left[(W - \sqrt{\mathbf{p}_T^2 + m^2} \cosh y)s - (P_L - \sqrt{\mathbf{p}_T^2 + m^2} \sinh y)t - i(\mathbf{P}_T - \mathbf{p}_T) \cdot u_T\right],
\end{aligned}
\tag{A6}
$$

and

$$
B = -\frac{1}{(2\pi)^4} \int_{\epsilon_0 - i\infty}^{\epsilon_0 + i\infty} ds \int_{\epsilon_1 - i\infty}^{\epsilon_1 + i\infty} dt \int du_T [F(s, t, u_T)]^n \exp[Ws - P_L t - i\mathbf{P}_T \cdot u_T].
\tag{A7}
$$

As elaborated further below [16,17], if these hadrons are emitted from a jet, it is a reasonable approximation to assume that $\langle p_T \rangle$ is not significant when compared to $\langle p_L \rangle$ as the hadrons are mostly aligned. This is in accordance with the scenario of a di-jet when the momentum component in the perpendicular direction of the jet is insignificant. In this regard, one relaxes the conservation of transverse momentum by assuming that $F(s, t, \mathbf{u}_T)$ does not depend on $\mathbf{u}_T$. We therefore replace $F(s, t, \mathbf{u}_T)$ by $F(s, t)$ in the above expressions. By noticing that the integrations in $\mathbf{u}_T$ become irrelevant and cancel out in the ratio, we find

$$
\left.\frac{d^3\bar{n}}{dy d\mathbf{p}_T}\right|_{n, W, P} \equiv \langle n_k \rangle \simeq n f(y, \mathbf{p}_T) dy d\mathbf{p}_T \frac{C}{D},
\tag{A8}
$$

where

$$
C = \int_{\epsilon_0 - i\infty}^{\epsilon_0 + i\infty} ds \int_{\epsilon_1 - i\infty}^{\epsilon_1 + i\infty} dt [F(s, t)]^{n-1} \times \exp\left[(W - \sqrt{\mathbf{p}_T^2 + m^2} \cosh y)s - (P_L - \sqrt{\mathbf{p}_T^2 + m^2} \sinh y)t\right],
\tag{A9}
$$

and

$$
D = \int_{\epsilon_0 - i\infty}^{\epsilon_0 + i\infty} ds \int_{\epsilon_1 - i\infty}^{\epsilon_1 + i\infty} dt [F(s, t)]^n \exp[Ws - P_L t].
\tag{A10}
$$

By assuming $m = 0$ in Equations (A9) and (A10), one readily obtains Equations (11) and (12) given in the main text.

References

1. Lee, T.D.; Wick, G.C. Vacuum Stability and Vacuum Excitation in a Spin 0 Field Theory. *Phys. Rev. D* **1974**, *9*, 2291. [CrossRef]
2. Lee, T.D. Abnormal Nuclear States and Vacuum Excitations. *Rev. Mod. Phys.* **1975**, *47*, 267. [CrossRef]
3. McLerran, L.; Samios, N. *TD Lee: Relativistic Heavy Ion Collisions and the Riken Brookhaven Center*; OSTI: Oak Ridge, TN, USA, 2006.
4. Rushbrooke, J.G. A review of low p(T) physics up to SPS collider energy (S**(1/2) = 540-GeV). In Proceedings of the 14th International Symposium on Multiparticle Dynamics, Granlibakken, CA, USA, 22–27 June 1985.
5. Dudek, J.; Ent, R.; Essig, R.; Kumar, K.S.; Meyer, C.; McKeown, R.D.; Meziani, Z.E.; Miller, G.A.; Pennington, M.; Richards, D.; et al. Physics Opportunities with the 12 GeV Upgrade at Jefferson Lab. *Eur. Phys. J. A* **2012**, *48*, 187. [CrossRef]
6. Accardi, A.; Albacete, J.L.; Anselmino, M.; Armesto, N.; Aschenauer, E.C.; Bacchetta, A.; Boer, D.; Brooks, W.K.; Burton, T.; Chang, N.-B.; et al. Electron Ion Collider: The Next QCD Frontier: Understanding the glue that binds us all. *Eur. Phys. J. A* **2016**, *52*, 268. [CrossRef]
7. Abramowicz, H.; Caldwell, A. HERA collider physics. *Rev. Mod. Phys.* **1999**, *71*, 1275. [CrossRef]
8. Hama, Y.; Plumer, M. Semi-inclusive rapidity distributions and a critical analysis of the concept of partition temperature. *Phys. Rev.* **1992**, *D46*, 160. [CrossRef]
9. Huang, K. *Statistical Mechanics*, 2nd ed.; Wiley: Hoboken, NJ, USA, 1987.
10. Chou, T.T.; Yang, C.N.; Yen, E. Single Particle Momentum Distribution at High-energies and Concept of Partition Temperature. *Phys. Rev. Lett.* **1985**, *54*, 510. [CrossRef]
11. Chou, T.T.; Yang, C.N. Remarks on Multiplicity and Momentum Distributions in e+ e- Collisions at W = 14-GeV, 34-GeV, 55-GeV, 100-GeV AND 120-GeV. *Phys. Lett.* **1988**, *B212*, 105. [CrossRef]
12. Darwin, C.G.; Fowler, R.H. Some refinements of the theory of dissociation equilibria. *Proc. Camb. Philos. Soc.* **1923**, *21*, 730.

13. Darwin, C.G.; Fowler, R.H. On the partition of energy Part II Statistical principles and thermodynamics. *Phil. Mag.* **1922**, *44*, 823. [CrossRef]

14. Guimaraes, F.B. Brief critical analysis of the Darwin–Fowler method. *arXiv* **2011**, arXiv:1109.1164.

15. Wilk, G.; Włodarczyk, Z. Interpretation of the Nonextensivity Parameter *q* in Some Applications of Tsallis Statistics and Lévy Distributions. *Phys. Rev. Lett.* **2000**, *84*, 2770. [CrossRef] [PubMed]

16. Urmossy, K.; Barnafoldi, G.G.; Biro, T.S. Generalised Tsallis Statistics in Electron-Positron Collisions. *Phys. Lett. B* **2011**, *701*, 111. [CrossRef]

17. Urmossy, K.; Barnaföldi, G.G.; Biró, T.S. Microcanonical jet-fragmentation in proton–proton collisions at LHC energy. *Phys. Lett. B* **2012**, *718*, 125. [CrossRef]

18. Aad, G.; Borjanović, I.; Božović-Jelisavčić, I.; Krstić, J.; Mamužić, J.; Mudrinić, M.; Popović, D.S.; Reljić, D.; Sijacki, D.; Simić, L.; et al. Charged-particle multiplicities in pp interactions measured with the ATLAS detector at the LHC. *New J. Phys.* **2011**, *13*, 053033. [CrossRef]

19. The ALICE Collaboration; Abelev, B.; Adam, J.; Adamová, D.; Adare, A.M.; Aggarwal, M.M.; Aglieri Rinella, G.; Agnello, M.; Agocs, A.G.; Agostinelli, A.; et al. Energy Dependence of the Transverse Momentum Distributions of Charged Particles in pp Collisions Measured by ALICE. *Eur. Phys. J.* **2013**, *C73*, 2662. [CrossRef]

20. CMS Collaboration; Khachatryan, V.; Sirunyan, A.M.; Tumasyan, A.; Adam, W.; Bergauer, T.; Dragicevic, M.; Erö, J.; Friedl, M.; Frühwirth, R.; et al. Transverse momentum and pseudorapidity distributions of charged hadrons in pp collisions at $\sqrt{s} = 0.9$ and 2.36 TeV. *J. High Energ. Phys.* **2010**, *2*, 041. [CrossRef]

21. CMS collaboration. Transverse-momentum and pseudorapidity distributions of charged hadrons in *pp* collisions at $\sqrt{s} = 7$ TeV. *Phys. Rev. Lett.* **2010**, *105*, 022002. [CrossRef] [PubMed]

22. The CMS collaboration; Chatrchyan, S.; Khachatryan, V.; Sirunyan, A.M.; Tumasyan, A.; Adam, W.; Bergauer, T.; Dragicevic, M.; Erö, J.; Fabjan, C.; et al. Charged particle transverse momentum spectra in *pp* collisions at $\sqrt{s} = 0.9$ and 7 TeV. *J. High Energ. Phys.* **2011**, *8*, 086. [CrossRef]

23. Tsallis, C. Possible Generalization of Boltzmann-Gibbs Statistics. *J. Statist. Phys.* **1988**, *52*, 479. [CrossRef]

24. Tsallis, C. Nonadditive entropy: The Concept and its use. *Eur. Phys. J.* **2009**, *A40*, 257. [CrossRef]

25. Tsallis, C. *Introduction to Nonextensive Statistical Mechanics*; Springer: New York, NY, USA, 2009.

26. Hagedorn, R. Multiplicities, pT distributions and the expected hadron to quark-gluon phase transition. *Riv. Nuovo Cim.* **1983**, *6*, 1. [CrossRef]

27. Brodsky, S.J.; Farrar, G.R. Scaling Laws at Large Transverse Momentum. *Phys. Rev. Lett.* **1973**, *31*, 1153. [CrossRef]

28. Brodsky, S.J.; Farrar, G.R. Scaling Laws for Large Momentum Transfer Processes. *Phys. Rev. D* **1975**, *11*, 1309. [CrossRef]

29. Matveev, V.A.; Muradian, R.M.; Tavkhelidze, A.N. Automodellism in the large—Angle elastic scattering and structure of hadrons. *Lett. Nuovo Cim.* **1973**, *7*, 719. [CrossRef]

30. Blankenbecler, R.; Brodsky, S.J.; Gunion, J.F. Analysis of Particle Production at Large Transverse Momentum. *Phys. Rev. D* **1975**, *12*, 3469. [CrossRef]

31. Schmidt, I.A.; Blankenbecler, R. Relativistic Interactions Between Nuclei. *Phys. Rev. D* **1977**, *15*, 3321. [CrossRef]

32. Arleo, F.M.C.; Brodsky, S.J.; Hwang, D.S.; Sickles, A.M. Higher-Twist Dynamics in Large Transverse Momentum Hadron Production. *Phys. Rev. Lett.* **2010**, *105*, 062002. [CrossRef]

33. Brodsky, S.; de Teramond, G.; Karliner, M. Puzzles in Hadronic Physics and Novel Quantum Chromodynamics Phenomenology. *Ann. Rev. Nucl. Part. Sci.* **2011**, *62*, 2082. [CrossRef]

34. Kodama, T.; Elze, H.T.; Aguiar, C.E.; Koide, T. Prethermalization and the effects of dynamical correlations. *EPL* **2005**, *70*, 439. [CrossRef]

35. Kodama, T.; Koide, T. Dynamical Origin of Power Spectra. *Eur. Phys. J. A* **2009**, *40*, 289. [CrossRef]

36. Osada, T.; Utyuzh, O.V.; Wilk, G.; Wlodarczyk, Z. Extended Gaussian ensemble or q-statistics in hadronic production processes? *Eur. Phys. J. B* **2006**, *50*, 7. [CrossRef]

37. Osada, T.; Wilk, G. Nonextensive hydrodynamics for relativistic heavy-ion collisions. *Phys. Rev. C* **2008**, *77*, 044903; Erratum in *Phys. Rev. C* **2008**, *78*, 069903. [CrossRef]

38. Jiang, K.; Zhu, Y.; Liu, W.; Chen, H.; Li, C.; Ruan, L.; Tang, Z.; Xu, Z. Onset of radial flow in p+p collisions. *Phys. Rev. C* **2015**, *91*, 024910. [CrossRef]

39. Wong, C.-Y.; Wilk, G. Tsallis fits to p_T spectra and multiple hard scattering in pp collisions at the LHC, *Phys. Rev.* **2013**, *D87*, 114007.